PROCEEDINGS OF SPIE

Optics and Photonics for Information Processing XIV

A. A. S. Awwal
K. M. Iftekharuddin
V. H. Diaz-Ramirez
A. Márquez
Editors

24 August – 4 September 2020
Online Only, United States

Sponsored and Published by
SPIE

Volume 11509

Proceedings of SPIE 0277-786X, V. 11509

Optics and Photonics for Information Processing XIV, edited by A. A. S. Awwal, K. M. Iftekharuddin, V. H. Diaz-Ramirez, A. Márquez, Proc. of SPIE Vol. 11509, 1150901 · © 2020 SPIE
CCC code: 0277-786X/20/$21 · doi: 10.1117/12.2581630

The papers in this volume were part of the technical conference cited on the cover and title page. Papers were selected and subject to review by the editors and conference program committee. Some conference presentations may not be available for publication. Additional papers and presentation recordings may be available online in the SPIE Digital Library at SPIEDigitalLibrary.org.

The papers reflect the work and thoughts of the authors and are published herein as submitted. The publisher is not responsible for the validity of the information or for any outcomes resulting from reliance thereon.

Please use the following format to cite material from these proceedings:
Author(s), "Title of Paper," in *Optics and Photonics for Information Processing XIV*, edited by A. A. S. Awwal, K. M. Iftekharuddin, V. H. Diaz-Ramirez, A. Márquez, Proceedings of SPIE Vol. 11509 (SPIE, Bellingham, WA, 2020) Seven-digit Article CID Number.

ISSN: 0277-786X
ISSN: 1996-756X (electronic)

ISBN: 9781510638242
ISBN: 9781510638259 (electronic)

Published by
SPIE
P.O. Box 10, Bellingham, Washington 98227-0010 USA
Telephone +1 360 676 3290 (Pacific Time) · Fax +1 360 647 1445
SPIE.org

Printed in the United States of America by Curran Associates, Inc., under license from SPIE.

Publication of record for individual papers is online in the SPIE Digital Library.

SPIE. DIGITAL LIBRARY
SPIEDigitalLibrary.org

Paper Numbering: *Proceedings of SPIE* follow an e-First publication model. A unique citation identifier (CID) number is assigned to each article at the time of publication. Utilization of CIDs allows articles to be fully citable as soon as they are published online, and connects the same identifier to all online and print versions of the publication. SPIE uses a seven-digit CID article numbering system structured as follows:

- The first five digits correspond to the SPIE volume number.
- The last two digits indicate publication order within the volume using a Base 36 numbering system employing both numerals and letters. These two-number sets start with 00, 01, 02, 03, 04, 05, 06, 07, 08, 09, 0A, 0B … 0Z, followed by 10-1Z, 20-2Z, etc. The CID Number appears on each page of the manuscript.

IMAGING ANALYSIS AND OPTICAL COMMUNICATIONS

POSTER SESSION

PROCEEDINGS OF SPIE

SPIEDigitalLibrary.org/conference-proceedings-of-spie

Polarization reconstruction of birefringence of the polycrystalline component of biological tissues with different damage durations

Litvinenko, A., Garazdyuk, M., Bachinskiy, V., Vanchulyak, O., Ushenko, A., et al.

A. Litvinenko, M. Garazdyuk, V. Bachinskiy, O. Vanchulyak, A. Ushenko, Yu. Ushenko, A. Dubolazov, L. Pidkamin, Bin Lin, Zhebo Chen, "Polarization reconstruction of birefringence of the polycrystalline component of biological tissues with different damage durations," Proc. SPIE 11509, Optics and Photonics for Information Processing XIV, 115090P (21 August 2020); doi: 10.1117/12.2568412

SPIE.

Event: SPIE Optical Engineering + Applications, 2020, Online Only

POLARIZATION RECONSTRUCTION OF BIREFRINGENCE OF THE POLYCRYSTALLINE COMPONENT OF BIOLOGICAL TISSUES WITH DIFFERENT DAMAGE DURATIONS

A.Litvinenko[1], M. Garazdyuk[1], V. Bachinsky[1], O. Vanchulyak[1], A.Ushenko[2] Yu.Ushenko[2], A.Dubolazov[2*], L.Pidkamin[2], Lin Bin[3], Chen Zhebo[3]

[1] Bukovinian State Medical University, 3 Theatral Sq., Chernivtsi, Ukraine, 58000
[2] Chernivtsi National University, 2 Kotsiubynskyi Str., Chernivtsi, Ukraine, 58012
[3] Reasearch Institute of Zhejiang University-Taizhou, 38 Zheda Road, Hangzhou, People's Republic of China, Zhejiang Province, 310027

a.dubolazov@chnu.edu.ua

ABSTRACT

By Mueller-matrix mapping of changes in the distribution of the magnitude of matrix invariants characterizing the degree of crystallization of histological sections of the brain, liver and kidney, the forensic medical criteria were determined and the interval for determining the damage duration of 24 hours with an accuracy of 45min. - 50 min. was established. For azimuthally invariant polarization mapping of changes in the distributions of Mueller-matrix invariants characterizing the optical activity of molecular complexes of histological sections of the brain, liver, and kidney, forensic medical criteria were developed for the first time and accuracy was improved to 35 min. - 40 min. in the interval for determining the damage duration period of 72 hours. For highly accurate objective determination of the damage duration in a long time interval (1 hour - 120 hours), a polarization tomography method has been developed (reproducing the distributions of birefringence of fibrillar networks of histological sections of internal organs), which provides an accuracy of 25 minutes. (1 hour - 24 hours) to 45 minutes (24 hours - 120 hours).

Keywords: polarimetry, birefringence, biological tissue, diagnostic.

1. INTRODUCTION

To represent the optical properties of an anisotropic medium using the formalism of the Mueller matrix, takes the following form [1-5]

$$\frac{d\{F\}(r)}{dr} = \{F\}(r)\{\mathrm{M}\}(r), \tag{1}$$

where $\{F\}(r)$ - Mueller matrix of a phase-inhomogeneous object in the plane of the partial layer located at a distance r.

It is known that for single-scattering (non-depolarizing) layers that convert the polarization of the probe radiation, the symmetry of the differential matrix $\{\mathrm{M}\}(r)$ is a combination of six elementary polarization properties [6-8]. These parameters fully characterize the amplitude (linear $LD_{0,90}$, $LD_{45,135}$ and circular CD dichroism) and phase (linear $LB_{0,90}$, $LB_{45,135}$ and circular CB birefringence) anisotropy of the biological layer

Optics and Photonics for Information Processing XIV, edited by A. A. S. Awwal, K. M. Iftekharuddin, V. H. Diaz-Ramirez, A. Márquez, Proc. of SPIE Vol. 11509, 115090P · © 2020 SPIE
CCC code: 0277-786X/20/$21 · doi: 10.1117/12.2568412

$$\{\mathrm{M}\}=\begin{Vmatrix} 0 & m_{12} & m_{13} & m_{14} \\ m_{21} & 0 & m_{23} & -m_{24} \\ m_{31} & -m_{32} & 0 & m_{34} \\ m_{41} & m_{42} & -m_{43} & 0 \end{Vmatrix}= \tag{2}$$

$$=\begin{Vmatrix} 0 & LD_{0,90} & LD_{45,135} & CD \\ LD_{0,90} & 0 & CB & -LB_{45,135} \\ LD_{45,135} & -CB & 0 & LB_{0,90} \\ CD & LB_{45,135} & -LB_{0,90} & 0 \end{Vmatrix}.$$

Here $LD_{0,90}$ and $LB_{0,90}$ - linear dichroism and birefringence for the direction of the optical axis $\rho = 0^0$; $LD_{45,135}$ and $LB_{45,135}$ - linear dichroism and birefringence for the direction of the optical axis $\rho = 45^0$; CD and CB - circular dichroism and birefringence.

The main "information" object of our studies of optical anisotropy of partially depolarizing biological layers will be the coordinate distribution of the value of the averaged elements by the average ($\langle m_{ik} \rangle$) of the differential matrix $\{\mathrm{M}\}$ [9-12].

Let us determine the algorithm for finding the elements of such a matrix by Stokes polarimetric mapping of polycrystalline networks of the sample under study, followed by obtaining a series of Mueller-matrix images $f_{ik}(x,y)$.

The polarization component $\mathrm{P}(r)$ of the logarithmic matrix algorithm $\Lambda(r)$ can be represented as follows

$$\langle\{\mathrm{M}\}\rangle = r^{-1}\begin{Vmatrix} 0 & (p_{12}+p_{21}) & (p_{13}+p_{31}) & (p_{14}+p_{41}) \\ (p_{21}+p_{12}) & 0 & (p_{23}-p_{32}) & (p_{24}-p_{42}) \\ (p_{31}+p_{13}) & (p_{32}-p_{23}) & 0 & (p_{34}-p_{43}) \\ (p_{41}+p_{14}) & (p_{42}-p_{24}) & (p_{43}-p_{34}) & 0 \end{Vmatrix}, \tag{3}$$

where

$$p_{ik} = \ln f_{ik}; \tag{4}$$

$$p_{ik} + p_{ki} = \ln(f_{ik} \times f_{ki}); \tag{5}$$

$$p_{ik} - p_{ki} = \ln\left(\frac{f_{ik}}{f_{ki}}\right). \tag{6}$$

Expression (3), taking into account relations (4) - (6), can be rewritten in the following analytical form, which characterizes the relationship between the polarization component $\langle\{\mathrm{M}\}\rangle$ of the differential matrix $\{\mathrm{M}\}$ and the Mueller matrix $\{F\}$

$$\left\langle\{\mathrm{M}\}\right\rangle = r^{-1}\begin{Vmatrix} 0 & \ln(f_{12}\,f_{21}) & \ln(f_{13}\,f_{31}) & \ln(f_{14}\,f_{41}) \\ \ln(f_{12}\,f_{21}) & 0 & \ln\left(\frac{f_{23}}{f_{32}}\right) & \ln\left(\frac{f_{24}}{f_{42}}\right) \\ \ln(f_{13}\,f_{31}) & \ln\left(\frac{f_{32}}{f_{23}}\right) & 0 & \ln\left(\frac{f_{34}}{f_{43}}\right) \\ \ln(f_{14}\,f_{41}) & \ln\left(\frac{f_{42}}{f_{24}}\right) & \ln\left(\frac{f_{43}}{f_{34}}\right) & 0 \end{Vmatrix}. \quad (7)$$

So, by direct Mueller-matrix mapping ($f_{ik}(x,y)$) of an optically anisotropic partially depolarizing biological layer, information on coordinate distributions $\left\langle\{m_{ik}(x,y)\}\right\rangle$ characterizing the averaged parameters of phase and amplitude anisotropy can be obtained.

The information obtained in this way is the basis for the polarization reproduction of the distributions of the average values of the linear and circular birefringence and the dichroism of the polycrystalline structure of the biological layer.

2. ALGORITHMS FOR RECONSTRUCTING THE DISTRIBUTIONS OF THE AVERAGE VALUES OF THE OPTICAL ANISOTROPY PARAMETERS OF BIOLOGICAL LAYERS

By a joint analysis of the relationships between the distributions $\left\langle\{m_{ik}(x,y)\}\right\rangle$ and $f_{ik}(x,y)$ on the basis of relations (1) - (3) and (7), we obtained algorithms for the polarization reproduction of the average values of the phase ($\left\langle\Delta n_{0;90}\right\rangle$; $\left\langle\Delta n_{45;135}\right\rangle$; $\left\langle\Delta n_{\otimes;\oplus}\right\rangle$) and amplitude ($\left\langle\Delta\mu_{0;90}\right\rangle$; $\left\langle\Delta\mu_{45;135}\right\rangle$; $\left\langle\Delta\mu_{\otimes;\oplus}\right\rangle$) anisotropy parameters of a partially depolarizing biological layer[12-16]

$$\left\langle\Delta n_{0,90}\right\rangle = \frac{\lambda}{2\pi r}\ln\left(\frac{f_{34}}{f_{43}}\right); \quad (8)$$

$$\left\langle\Delta n_{45;135}\right\rangle = \frac{\lambda}{2\pi r}\ln\left(\frac{f_{24}}{f_{42}}\right); \quad (9)$$

$$\left\langle\Delta n_{\otimes;\oplus}\right\rangle = \frac{\lambda}{2\pi r}\ln\left(\frac{f_{23}}{f_{32}}\right); \quad (10)$$

$$\left\langle\Delta\mu_{0,90}\right\rangle = \frac{\lambda}{2\pi r}\ln(f_{12}\,f_{21}); \quad (11)$$

$$\left\langle\Delta\mu_{45;135}\right\rangle = \frac{\lambda}{2\pi r}\ln(f_{13}\,f_{31}); \quad (12)$$

$$\left\langle\Delta\mu_{\otimes;\oplus}\right\rangle = \frac{\lambda}{2\pi r}\ln(f_{14}\,f_{41}). \quad (13)$$

Thus, the differential approach to the analysis of data obtained by the direct Mueller-matrix mapping method allowed us to obtain a set of algorithms (relation 8 – 13 for the polarization reproduction of the distributions of the average values of the linear and circular birefringence ($\left\langle\Delta n_{0;90}\right\rangle$; $\left\langle\Delta n_{45;135}\right\rangle$; $\left\langle\Delta n_{\otimes;\oplus}\right\rangle$) and dichroism ($\left\langle\Delta\mu_{0;90}\right\rangle$; $\left\langle\Delta\mu_{45;135}\right\rangle$; $\left\langle\Delta\mu_{\otimes;\oplus}\right\rangle$) parameters.

3. DIFFERENTIAL DIGITAL HISTOLOGICAL DIAGNOSIS OF THE DURATION OF THE FORMATION OF HUMAN LIVER DAMAGE BY METHOD OF THE TOMOGRAPHY OF CIRCULAR BIREFRINGENCE

On a series of fragments (1) - (3) fig. 1 shows tomograms of the optical activity of molecular complexes of liver tissue samples with different damage durations.

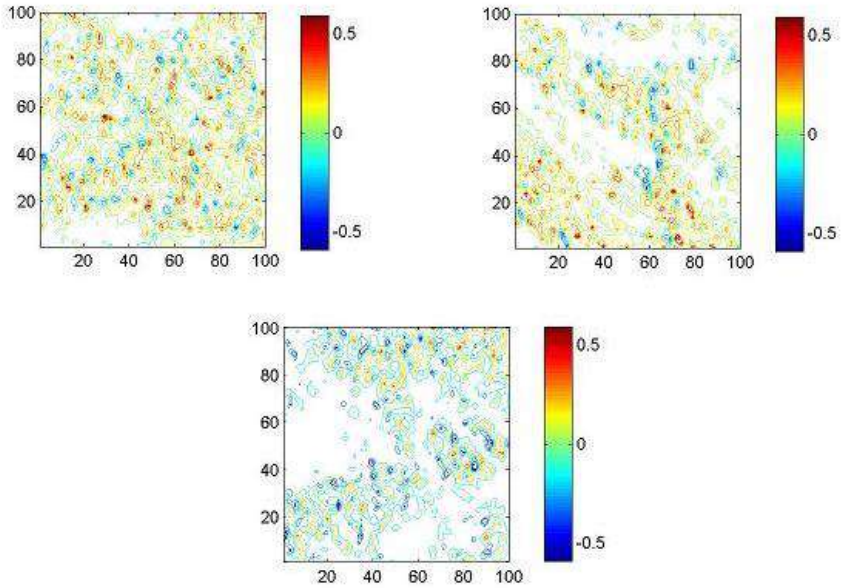

Fig. 1. Distribution maps of the magnitude of circular birefringence (x4) of histological sections of the liver of the deceased from the control group (1), research groups with different damage durations (6 hours - (2)) and (18 hours - (3))

An analysis of the transformation of the topographic structure of polarized reconstructed tomograms of circular birefringence of the totality of histological sections of the brain and intact and damaged liver (fig. 1) showed a decrease in the dispersion of the optical activity of liver samples while monotonously smoothing out fluctuations in circular birefringence with an increase in the damage duration of 6 hours and 18 hours (table 1)[17-20].

Table 1. Temporal dynamics of changes in statistical moments of the 1st - 4th orders of magnitude characterizing the distribution of the magnitude of the circular birefringence (4x) of histological sections of the liver

T, hours	**2**	**4**	**6**	**12**	**18**
SM_1 x10^{-3}	0,78 ± 0,034	0,71 ± 0,031	0,64 ± 0,023	0,51 ± 0,019	0,37 ± 0,012
p	p π 0,05				
SM_2 x10^{-3}	0,63 ± 0,024	0,55 ± 0,031	0,47 ± 0,019	0,31 ± 0,013	0,15 ± 0,008
p	p π 0,05				
SM_3	0,77 ± 0,032	1,08 ± 0,041	1,39 ± 0,057	2,07 ± 0,092	2,69 ± 0,11
p	p π 0,05				
SM_4	0,86 ± 0,035	1,26 ± 0,048	1,68 ± 0,067	2,38 ± 0,096	3,04 ± 0,12
p	p π 0,05				
T, hours	**24**	**48**	**72**	**96**	**120**
SM_1 x10^{-3}	0.23 ± 0,008	0,09 ± 0,004	0,11 ± 0,005	0,09 ± 0,006	0,11 ± 0,005
p	p π 0,05		p ϕ 0,05		
SM_2 x10^{-3}	0,06 ± 0,002	0,05 ± 0,013	0,04 ± 0,012	0,03 ± 0,012	0,02 ± 0,012
p	p π 0,05	p ϕ 0,05			
SM_3	3,18 ± 0,13	3,73 ± 0,14	4,34 ± 0,21	4,49 ± 0,25	4,52 ± 0,22

p	$p \pi 0{,}05$			$p \phi 0{,}05$	
SM_4	$3{,}76 \pm 0{,}016$	$4{,}47 \pm 0{,}22$	$5{,}17 \pm 0{,}24$	$5{,}33 \pm 0{,}25$	$5{,}41 \pm 0{,}24$
p	$p \pi 0{,}05$			$p \phi 0{,}05$	

Comparison of statistical monitoring data on changes in the topographic structure of the tomograms of the optical activity of the substance of brain samples and liver (table 1) revealed a similar scenario - an increase in the duration and an increase in the intervals of linear changes in the average, dispersion, asymmetry and excess.

The following temporal and dynamic characteristics of digital histology of tomograms of circular birefringence were determined:

- two intervals (1 hour - 24 hours and 24 hours - 48 hours) of a statistically significant ($p \pi 0{,}05$) linear change in the magnitude of the statistical moment of the first order, which characterizes the average distribution of circular birefringence up to 48 hours with a dynamic range of 0.93;
- 24 hours - a linear change in the magnitude of the statistical moment of the second order characterizing the variance of the dispersion of the values of the optical activity parameter with a dynamic range of 0.65;
- 72 hours - the duration of the treatment-sensitive interval (two linear sections 1 hour - 24 hours and 24 hours - 72 hours) changes in the magnitude of the statistical moments of the 3rd and 4th orders, characterizing the asymmetry and excess of the maps of circular birefringence.

Even greater functional capabilities in terms of greater duration diagnostic sensitivity method of digital histological polarization imaging optical activity of molecular complexes to determine the limitation of damage internal organs demonstrated by the use of large-scale (40x) reconstruction of the topographic distribution of magnitude of the circular birefringence of the liver tissue samples from a control and a set of research representative samples in a subsequent analysis of the data within the statistical approach, - fig. 2, table 2.

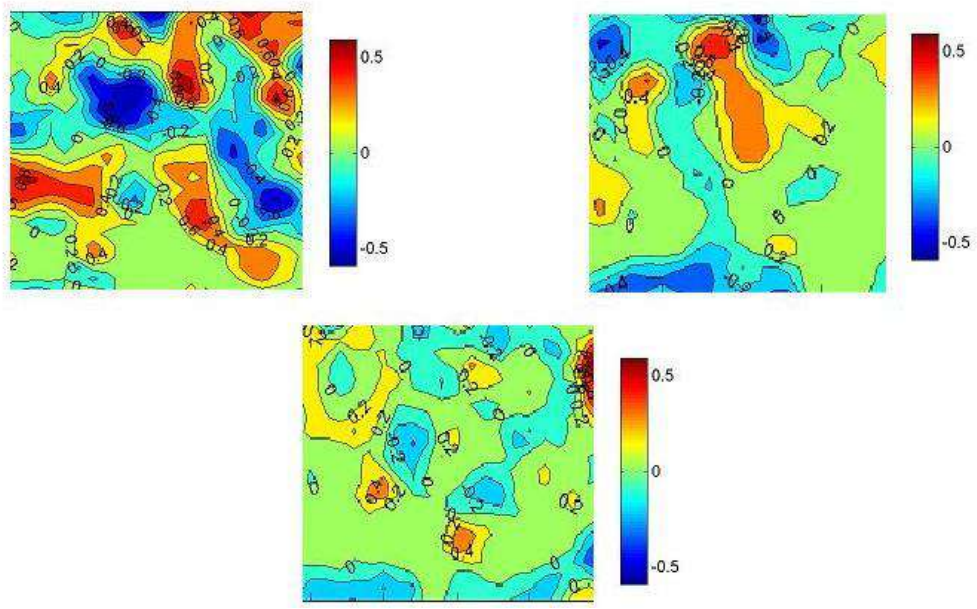

Fig. 2. Distribution maps of the magnitude of the circular birefringence (x40) of the histological sections of the liver of the deceased from the control group (1), research groups with different damage durations (6 hours - (2)) and (18 hours - (3)).

It is shown (table 2) that the use of a statistical analysis of the temporal dynamics of changes in topographic large-scale polarization tomograms of the degree of circular birefringence of optically active molecular complexes of samples of histological sections of the liver provided the maximum possible ranges (up to 120 hours) for detecting the age of damage by detecting linear intervals of variation in the average, dispersion , asymmetries and excesses characterizing the

distribution of birefringence magnitude of representative sets of samples from the control and the totality of research groups:

- 1st-order statistical moment characterizing the average distribution of the magnitude of circular birefringence - two linear intervals of 1 hour - 24 hours and 24 hours - 72 hours and a range of variation of the eigenvalues of 0.7;

Table 2. Temporal dynamics of changes in the statistical moments of the 1st - 4th orders characterizing the distribution of the magnitude of the circular birefringence (40x) of histological sections of the liver

T, hours	**2**	**4**	**6**	**12**	**18**
SM_1 x10^{-3}	0,72 ± 0,034	0,66 ± 0,031	0,59 ± 0,023	0,45 ± 0,019	0,32 ± 0,012
p	p π 0,05				
SM_2 x10^{-3}	0,59 ± 0,024	0,53 ± 0,031	0,47 ± 0,019	0,35 ± 0,013	0,23 ± 0,008
p	p π 0,05				
SM_3	0,83 ± 0,032	1,18 ± 0,041	1,53 ± 0,057	2,23 ± 0,092	2,93 ± 0,11
p	p π 0,05				
SM_4	0,95 ± 0,035	1,35 ± 0,058	1,78 ± 0,067	2,53 ± 0,011	3,34 ± 0,15
p	p π 0,05				
T, hours	**24**	**48**	**72**	**96**	**120**
SM_1 x10^{-3}	0.21 ± 0,008	0,08 ± 0,004	0,02 ± 0,005	0,03 ± 0,006	0,04 ± 0,005
p	p π 0,05			p ϕ 0,05	
SM_2 x10^{-3}	0,11 ± 0,004	0,05 ± 0,013	0,02 ± 0,012	0,03 ± 0,012	0,02 ± 0,012
p	p π 0,05			p ϕ 0,05	
SM_3	3,68 ± 0,15	4,33 ± 0,18	5,04 ± 0,22	5,74 ± 0,25	6,32 ± 0,28
p	p π 0,05				
SM_4	4,16 ± 0,16	4,96 ± 0,22	5,76 ± 0,26	6,63 ± 0,29	7,41 ± 0,34
p	p π 0,05				

- statistical moment of the second order, characterizing the dispersion of the scatter of a random value of optical activity - two linear intervals of 1 hour - 24 hours and 24 hours - 72 hours and a range of variation of eigenvalues of 0.57

- 3rd-order statistical moment, characterizing the asymmetry of the distribution of the magnitude of the circular birefringence of molecular complexes — two linear intervals of 1 hour to 24 hours. and 24 hours - 120 hours and a range of variation of eigenvalues of 5.49;

- a fourth-order statistical moment characterizing the excess of the distribution of the magnitude of circular birefringence - two linear intervals of 1 hour to 24 hours and 24 hours - 120 hours and a range of variation of eigenvalues of 6.46.

Table 3. Time intervals and accuracy of the method of reconstructing the optical activity of histological sections of internal organs

Brain				
Statistical moments	Interval, hours		Accuracy, min.	
Magnification	4x	40x	4x	40x
Average	1-24 24-48	1-24 24-72	35 45	30 35
Dispersion	1-24 24-48	1-24 24-72	35 45	30 35

Asymmetry	1-24 24-72	1-24 24-120	25 35	15 25
Excess	1-24 24-72	1-24 24-120	25 35	15 25
Liver				
Statistical moments	Interval, hours		Accuracy, min.	
Magnification	4x	40x	4x	40x
Average	1-24 24-48	1-24 24-72	40 50	35 45
Dispersion	1-24 24-48	1-24 24-72	40 50	35 45
Asymmetry	1-24 24-72	1-24 24-120	30 40	25 35
Excess	1-24 24-72	1-24 24-120	30 40	25 35
Kidney				
Statistical moments	Interval, hours		Accuracy, min.	
Magnification	4x	40x	4x	40x
Average	1-24 24-48	1-24 24-72	35 45	30 35
Dispersion	1-24 24-48	1-24 24-72	35 45	30 35
Asymmetry	1-24 24-72	1-24 24-120	25 35	20 30
Excess	1-24 24-72	1-24 24-120	25 35	20 30

CONCLUSIONS

A new original method of tomography of the optical activity of molecular complexes of tissues of internal organs of a person in a digital histological study of the age of damage to the tissues of the brain, liver and kidney over a time interval of 1 hour was developed. up to 120 hours.

A set of treatment-relevant relationships between temporal changes in the statistical structure of the topographic maps of circular birefringence of optically active molecular complexes of histological sections of human internal organs with different damage durations and variations in the average, dispersion, asymmetry and excess characterizing the distribution of the value of this anisotropy parameter has been determined.

The scenarios of changes in topographic tomograms of optical activity depending on the age of the damage are determined - the growth of this parameter is accompanied by a decrease in the statistical moments of the 1st (average) and 2nd (dispersion) orders, the statistical moments of the 3rd (asymmetry) and 4th (excess) orders, on the contrary, are growing.

A set of time ranges of linear change in the variation of the magnitude of statistical moments of the 1st - 4th orders of magnitude characterizing the distribution of tomographic data of the optical activity of molecular complexes of digital histology and the accuracy of determining the age of damage to internal organs:

1. Small-scale tomograms of circular birefringence (4x):
- average – 48 hours, accuracy 35 min. – 45 min.;
- dispersion – 48 hours, accuracy 35 min. – 45 min.;
- asymmetry – 72 hours, accuracy 25 хв. – 35 хв.;
- excess – 72 hours, accuracy 25 min. – 35 min.
2. Large-scale circular birefringence tomograms (40x):
- average – 72 hours, accuracy 30 min. – 35 min.;
- dispersion – 72 hours, accuracy 30 min. – 35 min.;

- asymmetry – 120 hours, accuracy 15 min. – 25 min.;
- excess – 120 hours, accuracy 15 min. – 25 min.

REFERENCES

[1]. Patterson M., Andersson-Engels S., Wilson B., Osei E., "Absorption-spectroscopy in tissue-simulating materials - a theoretical and experimental-study of photon paths," Appl. Opt. 34, 1995, 22-30.
[2]. Tuchin V., "Light scattering study of tissues," Physics-Uspekhi 40(5), 1997, pp. 495–515.
[3]. Tynes H. et al., "Monte Carlo and multicomponent approximation methods for vector radiative transfer by use of effective Mueller matrix calculations," Appl. Opt. 40(3), 2001, pp. 400–412.
[4]. Tower T., Tranquillo R., "Alignment Maps of Tissues: I. Microscopic Elliptical Polarimetry," Biophys. J., Vol. 81., 2001, pp. 2954-2963.
[5]. Tuchin V., "Handbook of optical biomedical diagnostics," SPIE Press, 2002, pp. 1110.
[6]. Wang L., Wu H.-I., "Biomedical Optics: Principles and Imaging," Wiley-Interscience, Hoboken, New Jersey 2007.
[7]. Boas D., Pitris C., Ramanujam N., Eds., "Handbook of Biomedical Optics," CRC Press, Boca Raton, London, New York 2011.
[8]. Vo-Dinh T., Ed., "Biomedical Photonics Handbook," 2nd ed., CRC Press, Boca Raton 2014.
[9]. Tuchin V., "Tissue Optics: Light Scattering Methods and Instruments for Medical Diagnostics," 3rd ed., Vol. PM 254, SPIE Press, Bellingham, Washington 2015.
[10]. Angelsky, O. V., Bekshaev, A. Y. A., Maksimyak, P. P., Maksimyak, A. P., & Hanson, S. G. (2018). Low-temperature laser-stimulated controllable generation of micro-bubbles in a water suspension of absorptive colloid particles. Optics Express, 26(11), 13995-14009.
[11]. Angelsky, O. V. (2007). Optical correlation techniques and applications. Optical correlation techniques and applications (pp. 1-270)
[12]. Angelsky, O. V., Ushenko, A. G., Pishak, V. P., Burkovets, D. N., Yermolenko, S. B., Pishak, O. V., & Ushenko, Y. A. (2000). Coherent introscopy of phase-inhomogeneous surfaces and layers. Paper presented at the Proceedings of SPIE - the International Society for Optical Engineering, 4016 413-418.
[13]. Angelsky OV, Bekshaev AY, Hanson SG, Zenkova CY, Mokhun II and Jun Z (2020) Structured Light: Ideas and Concepts. Front. Phys. 8:114.
[14]. Angelsky OV, Zenkova CY, Hanson SG and Zheng J (2020) Extraordinary Manifestation of Evanescent Wave in Biomedical Application. Front. Phys. 8:159.
[15]. Ushenko, Yu.A., Bachynsky, V.T., Vanchulyak, O.Ya., Dubolazov, A.V., Garazdyuk, M.S., Ushenko, V.A., "Jones-matrix mapping of complex degree of mutual anisotropy of birefringent protein networks during the differentiation of myocardium necrotic changes," (2016) Applied Optics, 55 (12), pp. B113-B119.
[16]. Ushenko, Yu.A., Dubolazov, A.V., Karachevtcev, A.O., Zabolotna, N.I., "A fractal and statistic analysis of Mueller-matrix images of phase inhomogeneous layers,"(2011) Proceedings of SPIE - The International Society for Optical Engineering, 8134, 81340P.
[17]. Ushenko, V.A., Dubolazov, A.V., "Correlation and self similarity structure of polycrystalline network biological layers mueller matrices images," (2013) Proceedings of SPIE - The International Society for Optical Engineering, 8856.
[18]. "Cassidy, "Basic concepts of statistical analysis for surgical research," Journal of Surgical Research 128,199-206 (2005).
[19]. C. S. Davis, Statistical methods of the analysis of repeated measurements, 744, New York: Springer-Verlag (2002).
[20]. A. Petrie, B. Sabin, Medical Statistics at a Glance, pp. 157, Blackwell Publishing (2005).